YKOB: Participatory Sensing–Based Road Condition Monitoring Using Smartphones Worn by Cyclist

Article *in* Electronics and Communications in Japan · February 2018

DOI: 10.1002/ecj.12027

5 authors, including:

Junji Takahashi
Kagoshima University
75 PUBLICATIONS **210** CITATIONS
SEE PROFILE

Yusuke Kobana
Aoyama Gakuin University
8 PUBLICATIONS **45** CITATIONS
SEE PROFILE

Naoya Isoyama
Nara Institute of Science and Technology
52 PUBLICATIONS **82** CITATIONS
SEE PROFILE

Yoshito Tobe
Aoyama Gakuin University
200 PUBLICATIONS **984** CITATIONS
SEE PROFILE

Electronics and Communications in Japan, Vol. 0, No. 0, 2017
Translated from Denki Gakkai Ronbunshi, Vol. 137-C, No. 4, April 2017, pp. 658–666

YKOB: Participatory Sensing-Based Road Condition Monitoring Using Smartphones Worn by Cyclist

JUNJI TAKAHASHI,[1] YUSUKE KOBANA,[2] NAOYA ISOYAMA,[2] YOSHITO TOBE,[2] and GUILLAUME LOPEZ[2]
[1]Kagoshima University, Japan
[2]Aoyama Gakuin University, Japan

SUMMARY

We propose a novel road monitoring system named YKOB (Your Kinetic Observation Bike) based on participatory sensing. YKOB collects acceleration signals using smartphones worn by cyclists, and analyzes the collected signals to investigate road surface condition. When a bicycle passes on a bump or a dimple, its wheels vibrate. The vibrations are transmitted to the smartphone via the bicycle frame or the cyclist body, and registered as acceleration signals. Conversely, by analyzing the acceleration signals we can estimate the road surface condition. There are mainly two research issues in this system. The first issue is that the acceleration registered at the smartphone includes cyclist motion signal as well as road surface signal. The second issue is that it is necessary to distinguish abnormality of road surface from artificial differences in level, such as a difference between streets and sidewalks. We developed a signal separation algorithm based on independent component analysis to solve the first issue. We also developed a bump classification algorithm using real mother wavelet. These two proposed algorithms were evaluated with 640 trials in total of experimental data conducted by eight cyclists. The classification accuracy of 0.68 validates the simultaneous utilization of our proposed algorithms. © 2018 Wiley Periodicals, Inc. Electron Comm Jpn, 0(0): 1–12, 2017; Published online in Wiley Online Library (wileyonlinelibrary.com). DOI 10.1002/ecj.12027

Keywords: independent component analysis; real mother wavelet; participatory sensing; maintenance of social infrastructure.

1. Introduction

Maintenance of social infrastructure is important but in reality has been insufficient due to its significant cost relative to the financial status of the administrative authority [1–3]. Roads in particular, accounting for huge volume share, are in need for an early detection system for road troubles and a low-cost sustainable inspection of irregular spots due to degradation over time although their urgency is lower than that of tunnels or bridges [4]. Effective measure for this issue is a concept of participatory sensing such as soliciting passersby to perform road monitoring for the authority.

The study on participatory sensing has been advanced in tandem with the diffusion of mobile terminals. One of the pioneering systems of this nature is WINFO [5] among others, which visualizes gusting areas by collecting data of opening and folding of umbrellas held in hands via mobile phone network. Such a system—in which the data captured via a personal mobile terminal are collected by servers, which in turn, feedback value-added information after analyzing the data—is dubbed "Participatory Sensing" by Burke and colleagues, and various issues have been sorted out [6] by this system. Later, it is also called "Crowdsensing" after its feature of utilizing the crowd capability, and now being discussed on its application to real problems after going through the investigations on system development [7], coverage [8], and node-to-node cooperation [9].

Among the applications of participatory sensing to a metropolitan environment survey, there is the noise map [10, 11] that connects a mobile device microphone to GPS positioning data as well as a temperature map, atmospheric pollution, traffic condition map, and so on, which have been organized by Christin and colleagues [12].

A system utilizing a probe car instead of a human is also available [13]. It predicts the traffic density around the car based on its acceleration/deceleration data and enables data sharing with other cars via intervehicle communication. There is yet another system using a public

transportation like a bus for sensing, and according to the research by Hasenfratz and colleagues, a streetcar is employed for investigating the radiowave reception condition in the city of Zurich [14].

Several studies are reported to monitor road surface conditions using participatory sensing. Erikkson and colleagues have succeeded in detecting irregular spots in the investigation of road surface conditions covering 9730 km stretch in Boston via 3-axis accelerometers mounted on seven cabs [15]. Mohan and colleagues propose a method of capturing acceleration data via a smartphone worn by a passenger in a car and judging road surface conditions by calculating the acceleration of the car after adjusting the gap between the terminal and the car attitude [16]. The former method, however, makes it difficult to monitor a vast area for a long period of time since it requires a dedicated apparatus despite its high precision detection of irregular road surface, and the latter poses an issue that its detection precision for irregular road surface is lower although it is easier to collect the monitoring data due to deployment of smartphones. Yagi has succeeded in detecting a road bump of about 2.4 cm by deploying combination of the individual merits of the two methods in which a smartphone is mounted on the dashboard of a car in an appropriate direction for capturing the acceleration signal [17]. Nonetheless, propagation of shocks in passing through road level differences varies by performance of car suspensions, which is considered to require fine-tuning of the parameters of detection algorithm for each and every car, and this needs to be further improved for collecting more sensing data.

It is an effective method as well for road monitoring to utilize bicycles of which traffic density is next to cars [18]. A bicycle that is lighter in weight and slower in velocity than a car can detect even a very minor road step since very few bicycles are equipped with suspensions. In addition, a bicycle is capable of monitoring detailed road surface conditions by going into a space where any car cannot access. The participatory sensing via bicycles is endowed with a probe bicycle [19], which assesses road surface conditions and traveling environment, BikeNet [20] logging a cyclist's condition and environment data during bike riding, and sBike [21] capturing the contexts during the riding. Every one of the above methods, however, needs to mount some sensor for measurement on a bicycle that would make it difficult to secure many participants. With the above background, we have been proposing YKOB (Your Kinetic Observation Bike) based on the premise of the participatory sensing, which inspects road surface conditions from the acceleration signal captured via smartphones held by the rider [22, 23]. The experiment in which a bike rider ran on the real road surface with a smartphone inserted in the trouser pocket [22], proved that the road surface signal can be extracted with high precision by applying the independent component analysis (ICA) for the issue of signal mixing of the observed signal with the signal of pedaling motion. On the other hand, it has been revealed that there is another issue that application of the threshold operation only to the road surface signal failed to distinguish an artificial road-step between a driveway and a sidewalk from the abnormal road-steps such as a bump and a dimple. In Ref. [23], in contrast, we confirmed that the newly developed algorithm to classify the three types of road-step, positive step, negative step, and convex step, based on the waveform feature of the road surface signal was effective in discriminating between the artificial road-steps and abnormal road-step. In this paper, the real mother wavelet (RMW) is augmented to enable discrimination of the four level differences including concave. In addition, the algorithms for extracting the road surface signal and classifying road-steps will be formulated in a more general format, and their efficacy will be demonstrated using data from multiple bike riders differing in their physical constitution.

This paper is composed of the following. Section 2 outlines the overall design of YKOB, and sorts out various issues based on the past experiment data. Furthermore, we show the result of questionaly survey on bike usage of students. Section 3 verifies, based on the experiment of concurrent measurement via smartphones worn at multiple positions of a single person, the magnitude of motion signal mixing for the above positions of the terminals. The extraction method for road surface signal via ICA is evaluated. In Section 4, RMWs corresponding to the four individual road-steps are configured from the road surface signals. Also, the algorithm, which classifies the road surface signals into the four types of step, PS (positive step), NS (negative step), CS (con-ved step), and CC (con-cave step) based on the similarity to the RMWs, are described. Section 5 verifies the efficacy of proposed method by applying the algorithms of proposed road surface signal extraction and of road-step classification to the observed signals captured by multiple bike riders varying in their physical constitution. The last Section 6 concludes this paper and mentions our future works.

2. YKOB System and its Issues

2.1 YKOB system

YKOB is a road monitoring system that collects road surface signals generated by a bike rider running on a road and performs inference of road conditions and detection of irregular spots from the analysis of compiled road surface signals. Its constituents are participants, servers, and road administrators (Fig. 1). Described below are the roles of individual constituents and various issues.

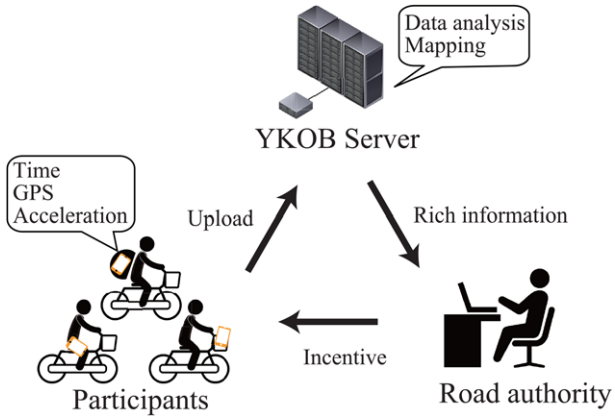

Fig. 1. Schematic of YKOB system, its components, and their relations. [Color figure can be viewed at wileyonlinelibrary.com]

2.1.1 Sensing by participants

What is required for participating YKOB monitoring are a smartphone and a bicycle only. The terminal device captures cruising data via 3-axis accelerometer and GPS receiver. The captured cruising data are uploaded to a server via wireless communication function of the device. The cruising data will be temporarily stored in the device when it is outside the network area, which will then be uploaded to the server as soon as the terminal enters the network area. A user shall be able to manually upload via PC the cruising data stored in the device.

It is an important matter to decide where to wear the terminal since the road surface asperity data are captured as acceleration signals. The probe bicycle [19] or sBike [21] suffers no noise effect due to the biker's motion since a terminal is mounted on the bike body. It, however, poses an issue of limiting the number of monitoring participants due to the fact that installation of a device to a bike is not prevalent at present. In YKOB, therefore, a device is allowed to be worn at a usual spot of a rider and the effect due to the wearing position is removed via signal processing. We conducted a research survey to find out on which part of the body an everyday biker wears the device. The details of the survey are presented in Section 2.2.

The sensing participant has to pass through any irregular spot riding on a bike for road surface monitoring. Two alternative methods are considered to be available for collecting the data, one to ask the sensing participant to pass through irregular spots intentionally for data collection, and the other to let the participant pass through irregular spots involuntarily for which data are collected. The former alternative demands some incentive to encourage the participants whereas the latter needs to have a larger number of sensing participants for statistical processes. In this paper, either one of the above alternatives can be accepted and therefore the discussion that follows will be focused on the data processing method.

2.1.2 Data analysis on server

The server analyzes the collected cruising data to perform inference of road surface conditions and detection of irregular spots. It infers the road surface conditions using the acceleration data of the cruising information, and if it detects any irregular spot, it is plotted on a map based on the corresponding GPS data. As argued above, the observed signal (acceleration data) obtained by a smartphone device suffer existence of the mixed signal of the road surface signal superimposed by the kinetic signal. There is still another problem that simple threshold value process alone cannot distinguish between an artificial level difference and an irregular one. The server, therefore, first extracts the road surface signals in accordance with the terminal installation position (Section 3.2). Then it infers the level difference topology by applying the level difference classification algorithm (Section 4.2) to the extracted road surface signal. From the classified level differences, the ascending and descending level differences are determined to be the artificial differences whereas convex and concave differences to be the irregular differences. The detail of the algorithms is provided in each section. It should be added that mapping of irregular spots of the detected road surface or calculation of the repair requirement are also the research subjects of significant importance, although this paper does not deal with them.

2.1.3 Prehension of road conditions by road administrator

The road administrator is represented by local government such as a nation, prefecture, city, town, county, and so on responsible for the road management.

Any irregularity is found efficiently through road monitoring via YKOB and repaired. The irregular spots are posted on the road failure data map that is publicized via Web to call for the attention of those concerned. The incentive planning for soliciting YKOB participants is also an important research subject although this paper does not deal with it.

2.2 Survey on bike usage

In order to investigate the wearing position of a smartphone device, a questionnaire survey was conducted with the members of College of Information Technology of our university. Out of the 202 respondents, 167 individuals who often ride a bicycle in daily life were classified as the bike users and their device wearing positions were tabulated.

Table 1. Result of the survey about smartphone location (multiple answers possible)

Smartphone location	No. of votes (people)	Percentage (%)
Front trouser pocket	110	65.9
Back trouser pocket	8	4.8
Front shirt pocket	12	7.2
Front basket of the bicycle	44	26.3
Shoulder bag, backpack	48	28.7
Mount on the bicycle with holder	3	1.8
Other	13	7.8

Table 1 exhibits the tabulation results. The device wearing positions in a descending order of vote count are; a front-pocket of a trouser, shoulder-bag/backpack, front basket of a bike, and chest-pocket of a shirt.

3. Tendency Analysis of Recorded Signal Depending on Wearing Position and Extraction of Road Surface Signal

3.1 Tendency analysis of recorded signal depending on wearing position

This survey is designed to investigate experimentally to what extent the motion signal of a bike rider mixes with the desired signal according to a smartphone wearing position. It has been clear in the preliminary experiment [23] that the acceleration signal captured at the rider's waist is most immune to the effect of bike rider's movement, and the road surface data emerge most intensely in the gravity direction component. We will, therefore, find out what magnitude of pristine road surface signal can be obtained for various wearing positions by comparing the gravity direction component (hereinafter waist signal) captured at the waist (p1) with the acceleration signals captured at other wearing locations.

The following wearing positions were selected for the survey based on the research result (Table 1) in Section 2.2; a trouser front-pocket (p2), shirt chest-pocket (p3), and front-basket (p4). Shoulder-bags/backpacks, despite their large share, were eliminated from this paper for the reason that they are suspected of providing data of lower reproducibility due to varying bag shapes and unstable device position inside the bag. The detailed experiment condition is provided in Section 5.

The 3-axis accelerometer data are captured for each of the wearing positions. In this experiment, correlation between all 3-axis accelerometer data and the waist signal is assessed, and the largest value of them is determined to be the correlation coefficient for the corresponding wearing position. Let the target acceleration signal be denoted by $x_{(t)}$, and the waist signal by $r_{(t)}$, then the correlation coefficient C is obtained by the equation below:

$$C(\tau) = \frac{\sum_{t=0}^{T} (r_{(t)} - \bar{r})(x_{(t+\tau)} - \bar{x})}{\sqrt{\sum_{t=0}^{T} (r_{(t)} - \bar{r})^2} \sqrt{\sum_{t=0}^{T} (x_{(t+\tau)} - \bar{x})^2}}, \quad C = \max C(\tau) \tag{1}$$

Here, the individual devices were synchronized with each other at the start of the measurement, but the offset was made using $\tau(-0.5 \leq \tau \leq 0.5)$ since the observed data were found to have a temporal gap of 0.1 ms maximum.

In the experiment, eight bike riders were instructed to pass through the four types of level difference as shown in Fig. 4 for 20 rounds yielding a total of 640 data units. An example of the obtained data and the correlation function are shown in Fig. 2 (1) to (4) and Fig. 2 (6), respectively. Table 2 exhibits the mean correlation coefficients between the respective data for the individual wearing positions of the device and the waist signal.

Table 2. The correlation coefficients between the signal on hip and signals on other locations

	Average of C of eight people × 20 trials data (SD)				
Location	PS	NS	CV	CC	Average of all bumps
p1	1.00	1.00	1.00	1.00	1.00 (0.00)
p2	0.60	0.62	0.55	0.48	0.56 (0.12)
p3	0.76	0.77	0.76	–	0.77 (0.07)
p4	0.33	0.26	0.37	–	0.32 (0.07)

As indicated in Table 2, the higher correlation between the shirt chest-pocket (p3) data and the waist signal (p1) seems to point to similarity between them, while the data for the trouser front-pocket (p2) and for the front-basket (p4) resulted in significantly larger deviations from the waist signal. The front-basket is exposed to the strong vibration propagated from the front wheel, whereas the rear wheel vibration is most responsible for the waist that is presumed to be attributable to the difference in the original road surface signal. In contrast, as can be seen in Fig. 2 (2), the kinetic signal mixing by pedaling is considered to be the primary culprit for the deviation of trouser front-pocket from the waist signal. This necessitates separation of the road surface signal and the kinetic signal.

3.2 Signal source separation by ICA

Wearing a device in a trouser front-pocket poses an issue of allowing a kinetic signal to mix with a road surface signal in the observed signal. In this section, we

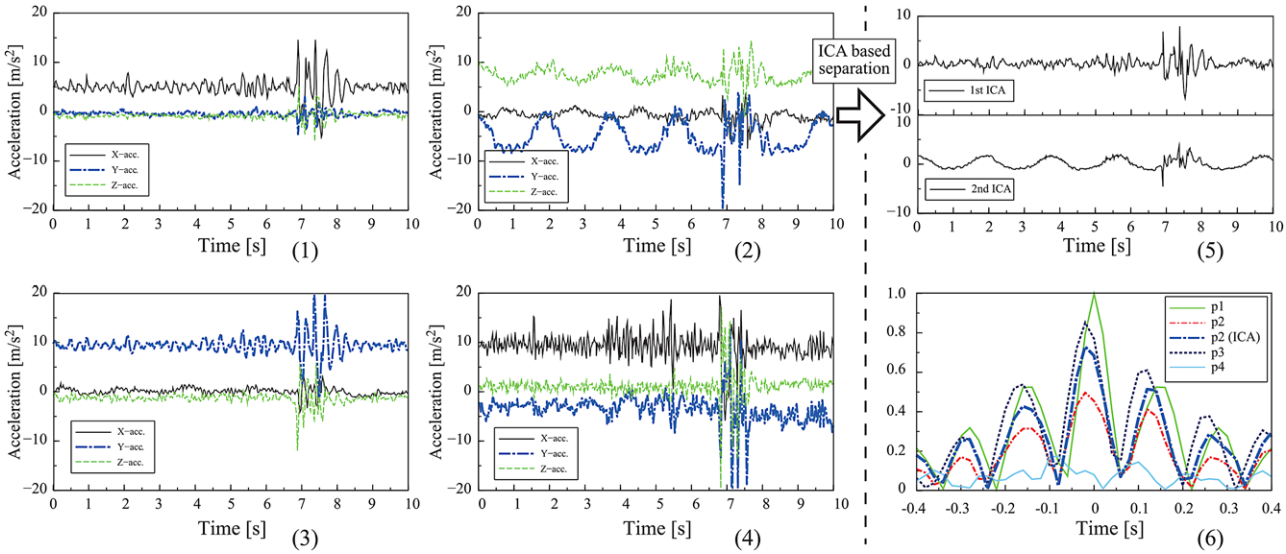

Fig. 2. Examples of registered acceleration data at respective locations, when a bicycle passes a positive step: (1) hip (p1), (2) front pants pocket (p2), (3) front shirt pocket (p3), (4) front basket of the bicycle, (5) separated signals after ICA based separation algorithm from the signals on p2, (6) correlation functions: $C(\tau)$ between the signal on hip (p1) and signals on other locations. [Color figure can be viewed at wileyonlinelibrary.com]

will outline the ICA, an effective solution for this issue, as well as FastICA, its accelerated algorithm, followed by our explanation of the road surface signal extraction via FastICA.

3.2.1 Independent component analysis

The ICA is a technique to deal with the blind source separation issue by inferring the source signal based on its statistical independency. Let the time or sample number be denoted by t, the source signal generated by l sources by $s = [s_1(t), \ldots, s_l(t)]^T$, and the m observed signals obtained by linear mixing of these signals by $x = [x_1(t), \ldots, x_m(t)]^T$. With the mixing matrix $\boldsymbol{A} \in \boldsymbol{R}^{m \times l}$, the relationship between the source signal and the observed signal is as follows:

$$\boldsymbol{x}(t) = \boldsymbol{A}\boldsymbol{s}(t). \tag{2}$$

The source signal s can be inferred by multiplying both sides of Eq. (2) by $\boldsymbol{A}^{-1}$ if the mixing matrix $\boldsymbol{A}$ is somehow obtained. In many cases, however, the signal propagation paths contain uncertainties and the mixing matrix itself is subject to temporal variation, which makes it difficult to clarify the mixing process precisely.

Making the separation matrix $\boldsymbol{W} \in \boldsymbol{R}^{n \times m}$ act on the observation signal $x(t)$ provides the separation signal $y = [y_1(t), \ldots, y_n(t)]^T$.

$$\boldsymbol{y}(t) = \boldsymbol{W}\boldsymbol{x}(t). \tag{3}$$

Here, it is known that the separation signal $\boldsymbol{y}$ becomes almost equal to the source signal $\boldsymbol{s}$ when $\boldsymbol{W}$ is chosen in the manner that the separation signal $\boldsymbol{y}$ approaches the utmost independence [24]. This is based on the central limit theorem that a signal distribution approaches a normal distribution as iteration of mixing the signal distribution increases.

3.2.2 FastICA

In this study, FastICA [25] will be used as the algorithm for executing ICA.

In FastICA, application of preprocesses of centralization and whitening to the data simplifies the computation thereby enabling faster convergence. The centralization is to apply the off-set to make the mean value of a signal distribution zero (0), and the whitening to normalize it with variance of 1 after uncorrelation of the data. Let $\boldsymbol{x}$ denote the centralized signal data, and $\boldsymbol{C}\boldsymbol{x} = E\{\boldsymbol{x}\boldsymbol{x}^T\}$ its covariance matrix. Further, let $\boldsymbol{D} = \mathrm{diag}\,(d_1 \ \ldots \ d_m)$ denote the diagonal matrix consisting of eigenvalue of $\boldsymbol{C}\boldsymbol{x}$, and $\boldsymbol{E} = (e_1 \ \ldots \ e_m)$ denote the matrix of norm 1 with eigenvector in its row. The whitening data z are expressed by equation below:

$$z = \boldsymbol{D}^{-1/2}\boldsymbol{E}^T\boldsymbol{x}. \tag{4}$$

As the signal independence evaluation criteria for this study, we employ the kurtosis, which is one of the non-Gaussian scales. The kurtosis relative to the component $y = \boldsymbol{w}^T z$ of the separation signal can be defined as:

$$\mathrm{kurt}(\boldsymbol{w}^T z) = E\{(\boldsymbol{w}^T z)^4\} - 3(E\{(\boldsymbol{w}^T z)^2\})^2 \tag{5}$$

utilizing the relationship $E\{z\} = 0$ via centralization. The kurtosis gradient must be considered for maximizing the kurtosis. It reaches the maximum level at the stable point of kurtosis gradient, which points to the $\boldsymbol{w}$ direction. Namely,

Table 3. Fast ICA algorithm for n-th components

1. Whitening $\boldsymbol{x}$ after centering to make z. Set $p \leftarrow 1$.
2. Initialize $\boldsymbol{w}_p$ with a random number, then $\boldsymbol{w}_p \leftarrow \boldsymbol{w}_p/||\boldsymbol{w}_p||$.
3. $\boldsymbol{w}_p \leftarrow E\{z(\boldsymbol{w}_p^T z)^3\} - 3\boldsymbol{w}_p$. (Update)
4. $\boldsymbol{w}_p \leftarrow \boldsymbol{w}_p - \sum_{j=1}^{p-1} (\boldsymbol{w}_p^T \boldsymbol{w}_j)\boldsymbol{w}_j$. (Orthogonalization)
5. $\boldsymbol{w}_p \leftarrow \boldsymbol{w}_p/||\boldsymbol{w}_p||$. if not converged, then go back to 3.
6. $p \rightarrow p + 1$. if $p \leq n$ then go back to 2.
7. $\boldsymbol{W} = [\boldsymbol{w}_1 \ \ldots \ \boldsymbol{w}_n]^T$.
8. Calculate $\boldsymbol{y} = \boldsymbol{W}x$.

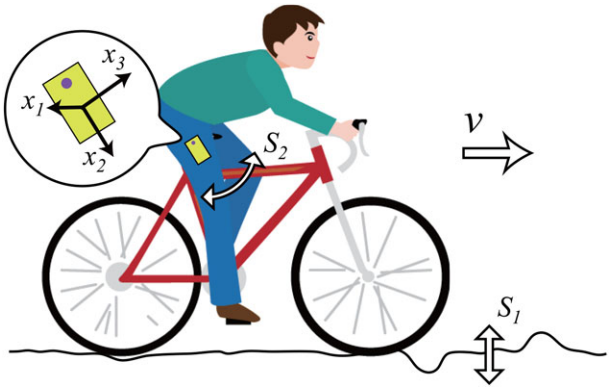

Fig. 3. The ICA observation model on YKOB. [Color figure can be viewed at wileyonlinelibrary.com]

the $\boldsymbol{w}$ that maximizes the kurtosis is obtained by iterating computation of the kurtosis gradient as a new $\boldsymbol{w}$. The $\boldsymbol{w}$ update expression is obtained as follows based on the premise that for the whitening data, $E\{(\mathbf{w}^T\mathbf{z})^2\} = ||\boldsymbol{w}||^2$, and $||\boldsymbol{w}|| = 1$ always holds true for dividing $\boldsymbol{w}$ by its norm.

$$\boldsymbol{w} \leftarrow E(z(\boldsymbol{w}^T z)^3) - 3\boldsymbol{w}\,. \tag{6}$$

Table 3 demonstrates FastICA procedure, with the observed signal $\boldsymbol{x}$ as input, to output the separation signal $\boldsymbol{y}$ consisting of multiple independent components.

3.2.3 Extraction of road surface signal via FastICA

The ICA observation model schematic is shown in Fig. 3. YKOB assumes the two types of signal, the road surface signal bearing concave/convex road surface information: $s_1(t)$, and the pedaling signal generated by the rider's leg movement: $s_2(t)$. Their respective source signals are captured by a smartphone device that propagate through the bike wheel, frame, and rider's body after they are generated. These two source signals, which cannot be measured in direct manner, are captured as the observed signal $\boldsymbol{x}$ via each axis of accelerometer of the terminal device after going through unknown mixing processes.

In Fig. 2 (2), it can be confirmed that the observed signal manifests the mixture of road surface and pedaling signals. The outcome of applying FastICA algorithm shown in Table 3 with the isolation signal count of $n = 2$ to this observed signal is presented in Fig. 2 (5).

Here, we classified the one with the larger kurtosis kurt(y) as the first independent component (y_1) and smaller kurtosis as the second independent component (y_2). The waveform presumably caused by the impact generated when passing through the level difference emerged in y_1. On the other hand, about 2-s cyclic waveform seemingly coming from the pedaling signal manifested itself intensely in y_2. It can be presumed from the above that the observed signal was successfully separated into the two types of signal in such a way that the road surface signal emerged explicitly in y_1 and the pedaling signal in y_2. In this example, the preseparation correlation was $C = 0.487$, and the postseparation correlation was $C_{ICA} = 0.717$. The ICA application to other data will be discussed in Section 5.2.1.

4. Inferring Road Surface Condition

4.1 Type of road step and acceleration signal

A roughness index determines flatness of a road but is a macroscopic index to be defined for a certain interval of a road, and thus is not appropriate for a microscopic condition like sporadic road surface irregularities, which this paper zeroes in on. It is more useful for monitoring the road surface irregularities to have ability to identify an irregular spot and infer its shape, dimension, and so on. It is particularly desirable to be able to infer the shape of a road step for discriminating an artificial step like the one between a driveway and a sidewalk in the bike ride space from the irregular road step such as cracks, depressions, bumps, and so on. In this paper, therefore, we will attempt to classify the basic shape of road step into four types, PS, NS, CV, and CC, as shown in Fig. 4. On the actual road surface, PS and NS are found as artificial road step between driveways and sidewalks whereas CS and CC as bumps, depressions, and cracks. Classifying the shape of road step into any of the four categories, PS, NS, CV, or CC, enables judgment on an artificial difference or any road surface irregularity.

Figure 5 shows the acceleration signal captured at the rider's waist position (p1) when passing through the road step exhibited in Fig. 4. On these signals, twice the waveforms were found similar to each other like the peaks and troughs, a, b, c and d, e, f of the signal waveform passing through PS. The distance is $\Delta d_{a\text{-}d} = 1100$ mm, for the time interval over a to d is $\Delta t_{a\text{-}d} = 0.4$ s, and the bike velocity is $v = 9.9$ km/h.

This distance is equal to the front-rear wheel stretch of the bike, $wb = 1100$ mm (Fig. 9), which is supposed to indicate that the leading waveform of the above two

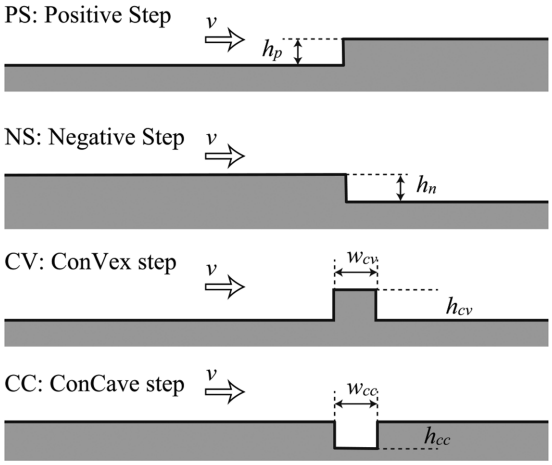

Fig. 4. Four types of steps.

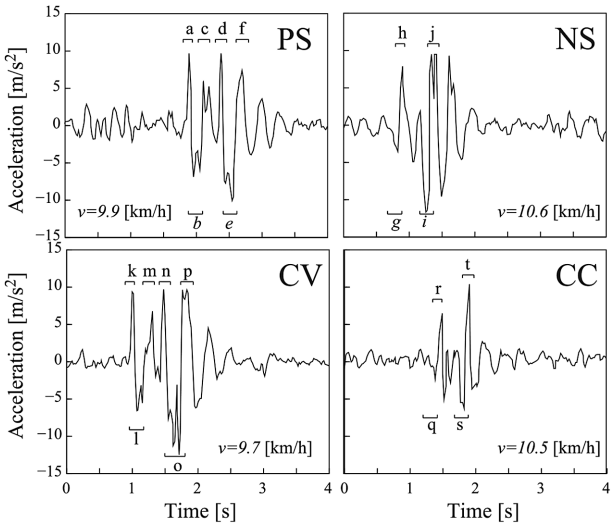

Fig. 5. Actual registered road surface signals.

Table 4. Relation between road surface signal and wheel condition

Wheel condition	PS	NS	CV	CC
Front wheel, tip up	*a*	–	*k*	–
Front wheel, free fall	*b*	g	*l*	*q*
Front wheel, landing	*c*	*h*	*m*	*r*
Rear wheel, tip up	*d*	–	*n*	–
Rear wheel, free fall	*e*	*i*	*o*	*s*
Rear wheel, landing	*f*	*j*	*p*	*t*

corresponds to the front-wheel condition and the trailing one to the rear-wheel (Table 4). The signal waveform varies by a type of road step as explained above and thus it is presumed to be possible to infer the shape of road step from the waveform.

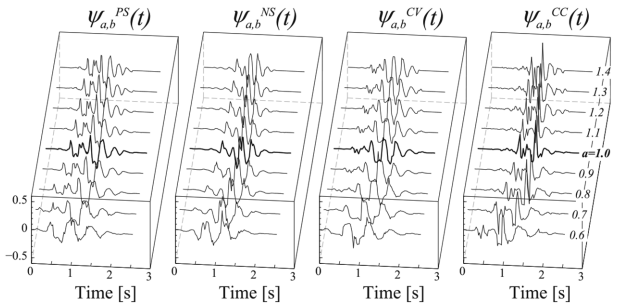

Fig. 6. Generated RMW family.

4.2 Classification of road step using RMW

As argued in the preceding section, individual measurement signal waveforms show their distinct tendencies depending on the shape of road step. In this paper, the signal waveform tendencies are expressed by using RMW [26] for classifying the unknown signal via assessment of its similarity to RMW. We will first explain how to create the RMWs followed by description of the road step classification algorithm based on the assessment of similarity to RMW.

4.2.1 Creating RMW

The RMW $\psi^i(t)$ ($i = PS,NS,CV,CC$) corresponding to the respective road step is created from the acceleration signal in Fig. 5. The RMW will be created in the following procedure.

1. Cropping RMW candidate signal with sample size p.
2. Applying Hamming window function.
3. Generating function set $\psi_{a,b}(t)$ via scale a adjustment

$$\psi_{a,b}(t) = a^{-\frac{1}{2}}\psi\left(\frac{t-b}{a}\right). \tag{7}$$

4. Normalization with norm $||\ \psi_{a,b}(t)||$ to become 1.

In this paper, the function set was configured with sample size $p = 128$ (2.56 s) using the nine elements $a = 0.6$, …, 1.4. The range of a was determined as above since the bike velocity was set between 8.0 km/h and 12 km/h in the experiment. The generated function set ${\psi^i}_{a,b}(t)$ is exhibited in Fig. 6.

4.2.2 Road step classification by RMW

We will explain the classification method for unknown time series signal $f(t)$. First, the correlation between

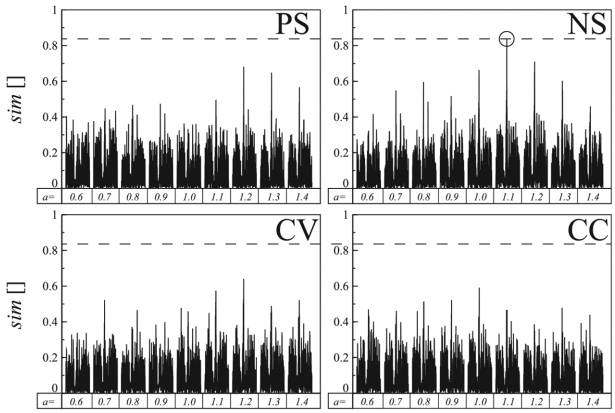

Fig. 7. The correlation between $f(t)$ and $\psi i\ a,b(t)$.

the unknown signal $f(t)$ and function set ${\psi^i}_{a,b}(t)$ is obtained by the equation below:

$$w(a,b)^i = \int_{-\infty}^{\infty} f(t)\psi^i_{a,b}(t)dt. \tag{8}$$

The obtained maximum value of the correlation function $w^i(a,\ b)$ is defined as the similarity *sim,* and the i value of ${\psi^i}_{a,b}(t)$ providing the maximum *sim* among all the function sets is chosen as the assessment result for that particular signal. As an example, Fig. 7 illustrates the computation result for the correlation between the signal captured during passage through NS and the function set shown in Fig. 6. The *sim* became maximum when $i = NS$ of which assessment result shall be NS. Here, since a is made active as the adjustment parameter for the temporal scale, it is possible to calculate the correlation properly even when the original sample signal of RMW differs from the bike velocity of evaluation target signal.

5. Experiment

5.1 Experimental environment and condition

We conducted some experiments to evaluate the precision of road-signal extraction via ICA and the accuracy of road-step classification algorithm via RMW. Figure 8 shows the experimental setup of the courses with each road-step. The magnitude of road-step was set to $h_p = 46$, $h_n = 46$, $h_{cv} = 53$, $w_{cv} = 98$, $h_{cc} = 58$, $w_{cc} = 200$ mm, respectively. The bike ride was hardly affected by the lateral G due to lower bike velocity ranging from 8.0 km/h to 12.0 km/h despite the existence of the course with a gentle curve.

Figure 9 shows the bicycle, smartphone devices, and various measurement apparatus used in the experiment. From the device (Master) mounted on the bike handlebar, the log file name for the device worn at each of the four measurement places p1, p2, p3, and p4 is entered and the data logging is started. The sampling interval for the acceleration signal is set to 20 ms for all the devices without exception. The SIGMAROX5.0, which calculates the velocity based on the rotation frequency of the front wheel, was used for measuring the bike velocity. The eight bike riders varying in their physical constitution (height: 165 cm to 180 cm, weight: 50 kg to 80 kg) participated in the experiment and passed through each of the four types of road-step 20 times per person yielding a total of 640 data.

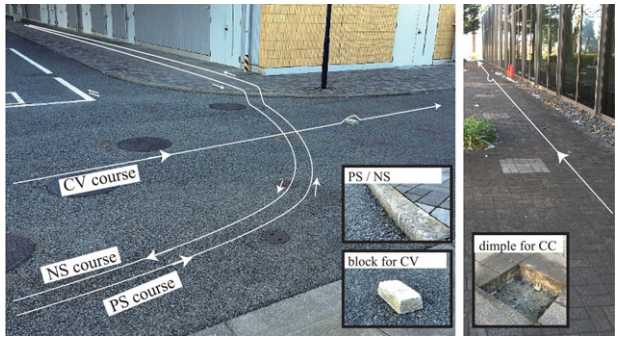

Fig. 8. The courses and bumps used for the experiment. [Color figure can be viewed at wileyonlinelibrary.com]

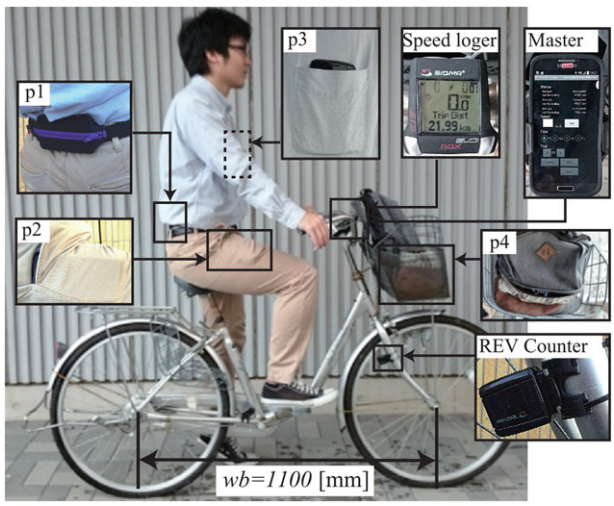

Fig. 9. The bicycle and the equipment positioning for the experiment. [Color figure can be viewed at wileyonlinelibrary.com]

5.2 Experimental results

5.2.1 Results of signal extraction via ICA

We extracted the road surface signal from the acceleration signal captured at the trouser pocket via signal separation algorithm based on proposed ICA. We then derived the correlation between the extracted road surface signal (p2 after ICA) and the waist signal (p1). Table 5 summarizes the mean values for each of the road-step and

Table 5. The correlation coefficients between the signal at p1 and p2 after ICA-based separation

	Average of C of eight people × 20 trials data (SD)				
Location	PS	NS	CV	CC	Average of all bumps
p2 (after ICA)	0.66	0.67	0.60	0.58	0.63 (0.11)

Table 6. Classification result: one versus one (p1)

Accuracy		True condition				
0.83		PS	NS	CV	CC	Precision
Prediction condition	PS	142	0	39	8	0.73
	NS	0	143	8	10	0.89
	CV	17	8	110	3	0.80
	CC	1	4	3	139	0.95
Recall		0.89	0.89	0.69	0.87	

the entire calculation results out of the whole data. The overall average of the correlation coefficients rose to 0.63 from 0.56, which was obtained before application of the separation algorithm. It has been verified from the above that the road surface signal was successfully extracted via proposed ICA algorithm from the observed signals of the motion and road surface in mixture.

5.2.2 Results of road-step classification via RMW

For classifying the road surface shape, there are two alternatives, the first is "one versus one" to assess the correlation between RMW, which is to be prepared for each rider, and the evaluating signal, and the second is "one versus all" to assess the same correlation between RMW for one single rider and the evaluating signal of all the riders. It should be noted that there are three types of the evaluating signal, the waist signal (p1), road surface signal (p2 after ICA) extracted from the signal captured at the trouser pocket via separation algorithm based on ICA, and the signal captured at the chest pocket (p3). A total of five different analyses were made based on the above combinations.

The result for each of the above cases is presented in Tables 6 to 10. According to the "one versus one (p1)" outcome in Table 6, the overall accuracy rate turned out to be 0.83, which is so high as to prove the effectiveness of level difference classification using RMW. Also in the case of "one versus one (p2 after ICA)" result in Table 7, the overall accuracy rate reached as high as 0.68 boasting of its sufficient performance for a parallel deployment of the signal separation algorithm based on ICA and the road-step classification algorithm via RMW.

Nonetheless, some areas were found for improvement in which the level difference of CV was often misjudged as PS.

Table 7. Classification result: one versus one (p2 after ICA)

Accuracy		True condition				
0.68		PS	NS	CV	CC	Precision
Prediction condition	PS	122	6	54	12	0.63
	NS	8	118	32	11	0.70
	CV	14	10	64	5	0.69
	CC	16	26	10	132	0.72
Recall		0.76	0.74	0.40	0.83	

Table 8. Classification result: one versus all (p1)

Accuracy		True condition				
0.74		PS	NS	CV	CC	Precision
Prediction condition	PS	104	3	69	10	0.56
	NS	14	141	6	4	0.85
	CV	41	12	84	2	0.60
	CC	1	4	1	144	0.96
Recall		0.65	0.88	0.53	0.90	

Table 9. Classification result: one versus all (p2 after ICA)

Accuracy		True condition				
0.60		PS	NS	CV	CC	Precision
Prediction condition	PS	94	13	68	9	0.51
	NS	21	113	32	18	0.61
	CV	34	21	53	10	0.45
	CC	11	13	7	123	0.80
Recall		0.59	0.71	0.33	0.77	

Table 10. Classification result: one versus all (p3)

Accuracy		True condition				
0.62		PS	NS	CV	CC	Precision
Prediction condition	PS	84	3	57	0	0.58
	NS	4	117	6	0	0.92
	CV	72	40	97	0	0.46
	CC	0	0	0	0	–
Recall		0.53	0.73	0.61	–	

In the "one versus all" scheme as well, the accuracy rates were as high as p1: 0.74, p2 after ICA: 0. 60, and p3: 0.62, but the misjudgment ratio increased across the board. This is considered to be attributable to the insufficient ability of RMW created this time for each road-step to absorb the individual differences of riders including their physical constitution, behavioral characteristic, and so on.

6. Conclusion

In this paper, we have proposed a road monitoring system named YKOB as a low-cost monitoring scheme for the tremendous volume of roads. The comprehensive YKOB system is composed of participants, servers, and road administrators. In this paper, focusing on the collection of cycling information from the participants and analyses via servers, we have succeeded in solving the issue that the acceleration signal captured via smartphones was superimposed not only by the road surface signal but by the bike rider's motion signal, and another issue of inferring the shape of road-step passed over by the bike based on the extracted road surface signal. In dealing with the former task, we developed the signal separation algorithm based on the ICA and succeeded in extracting only the road surface signal out of the mixed signal of pedaling and road surface signals. In terms of the correlation with the waist signal that is closest to the road surface signal, it showed an improvement from 0.56 to 0.63 due to the extraction effect. For the latter task, the road-step classification algorithm was developed using the RMW. This method is capable of detecting the target signal of high similarity by creating the mother wavelet based on the real signal. In the experiment evaluating the classification performance for the four types of road-step, PS, NS, CV, and CC, the accuracy rate of the "one versus one" scheme yielded 0.83 based on a total of 640 data collected from eight bike riders. Also in case of the signal isolated via proposed ICA algorithm, the accuracy rate reached as high as 0.68 endorsing its sufficient performance for a parallel deployment of both the methods.

As for the future issues, improvement of the accuracy rate for the "one versus all" method is the first priority. To deal with this, it is essential to establish universal RMW encompassing different bike types or varying tire pressure conditions as well as avoiding any effect of the physical constitution of bike riders or their behavioral characteristic. We, therefore, plan to collect data from many more participants on the actual roads. Furthermore, we will also develop a mapping of road surface anomalous spots, estimate repair requirement urgency, prepare an incentive plan for soliciting more participants, and so on. In this paper, the road steps used in the experiment were fixed to a rather large scale in order to comply with its primary objective of confirming the principle of the proposed method. In the future, we intend to develop a system capable of verifying the minimum dimension of road bump that is detectable by the proposed method, clarifying the relationship between the scale of road-step and the acceleration signal, and estimating the scale of road-step from the acceleration signal.

REFERENCES

1. Matsuda W. Pursuing establishment of road maintenance cycle—Interim summary report by road maintenance technical subcommittee. Public Works Manag J 2013.
2. Kishi Y. Bicycle accidents and negligence of road installation administration. North Intersect 2009;25.
3. Road Traffic Management Section, Road Transport Bureau, MLIT. Bicycle rider toppling accident caused by potholes on a road during road-race bike cruising in mountainous area. Road Administration Seminar on Dispute over Road Management Negligence, No. 56, 2013.
4. Yorifuji M, Tokida K. Repairing damages due to major level differences caused by earthquake, and management and deployment of traffic opening, p 67, 2007.
5. Sasaki K, Inoue U, Tobe Y. WINFO: A human-assisted sensor network, Proceedings of International Workshop on Networked Sensing Systems, 2005.
6. Burke J, Estrin D, Hansen M, Parker A, Ramanathan N, Reddy S, Srivastava MB. Participatory sensing. Proceedings of Workshop on World-Sensor-Web (WSW'06): Mobile Device Centric Sensor Networks and Applications, 2006.
7. Imura K, Nakazawa J, Tokuda H. A development tool for human as a sensor service. IEICE 2011:27–32.
8. Ahmed A, Yasumoto K, Yamauchi Y, Ito M. Probabilistic coverage methods in people-centric sensing. J Inform Process 2011;19:473–490.
9. Thepvilojanapong N, Konomi S, Tobe Y. A study of cooperative human probes in urban sensing environments. IEICE Trans Comm 2010;E93-B(11):2868–2878.
10. Stevens M, D'Hondt E. Crowdsourcing of pollution data using smartphones. Proceedings of UbiComp'10, 2010.
11. Meurisch C, Planz K. Noisemap—Discussing scalability in participatory sensing. Proceedings of ACM SenseMine'13, 2013.
12. Christin D, Reinhardt A, Kanhere S, Hollick M. A survey on privacy in mobile participatory sensing applications. J Syst Software 2011.
13. Sato M, Ishida T, Horiguchi R, Shimizu K, Haruta H, Wada K, Uehara K, Murai J. Evaluation of roadc

information generation algorithm for decentralized probe vehicle system. Trans Inform Process Soc Jpn 2008;49(1):253–264.
14. Hasenfratz D, Sturzenegger S, Saukh O, Thiele L. Spatially resolved monitoring of radio-frequency electromagnetic fields. Proceedings of ACM SenseMine'13, 2013.
15. Eriksson J, Girod L, Hull B, Newton R, Madden S, Balakrishnan H. The pothole patrol: Using a mobile sensor network for road surface monitoring. Proceedings of the International Conference on Mobile Systems, Applications, and Services, 2008.
16. Mohan P, Padmanabhan VN, Ramjee R. Rich monitoring of road and traffic conditions using mobile smartphones. ACM SenSys'08, p 323–336, 2008.
17. Yagi K. Road bump detection method using accelerometer on smartphone. The 9th ITS Symposium, 2010.
18. Japan Bycycle Promotion Institute. Research Report on Bicycle Ownership Status in 2012 (Summary), 2013.
19. Yamanaka H, Namerikawa S, Nakajima Y, Makimura K. Development of probe bicycles and evaluation of cycling paths. JSTE J Traffic Eng 2003;23(1):157–160.
20. Eisenman SB, Miluzzo E, Lane ND, Peterson RA, Ahn GS, Campbell A. BikeNet: A mobile sensing system for cyclist experience mapping. ACM Trans Sensor Networks 2009;1(6).
21. Saito Y, Sugo K, Aida H, Thepvilojanapong N, Tobe Y. sBike: Acquisition of person's state riding a bicycle with mobile sensing for participatory sensing. J Inform Process Soc Jpn 2012;53(2):770–782.
22. Kobana Y, Takahashi J, Usami I, Kitsunezaki N, Tobe Y, Guillaume L. Inspection of road status by bicycle riders: Basic principle and preliminary experiments, Mobile Computing and Pervasive System Workshop at The 71st Research Presentations. J Inform Process Soc Jpn 2014.
23. Takahashi J, Kobana Y, Tobe Y, Lopez G. Classification of steps on road surface using acceleration signals. Proceedings on International Workshop on Web Intelligence and Smart Sensing, 2015.
24. Nemoto I, Kawakatsu M. Details of new independent component analysis signal world. Tokyo Denki University Press; 2005.
25. Hyv¨arinen A, Oja E. A fast fixed-point algorithm for independent component analysis. Neural Comput 1997;9(7):1483–1492.
26. Zhang Z, Ikeuchi H, Ishi H, Horihata S, Imamura T, Miyake T. Real-signal mother wavelet and its application detection of abnormal signal designing average complex real-signal mother wavelet and its application. Trans Jpn Soc Mech Eng Series C 2007;73:730.

AUTHOR

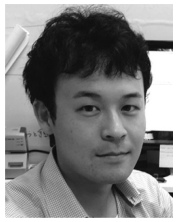

Junji Takahashi (nonmember) completed Micro-Nano Mechanical Science and Engineering from Graduate School of Nagoya University in 2010. He is a Doctor of Engineering. He is an Associate Professor at Department of Mechanical Engineering, Graduate School of Science and Engineering, Kagoshima University from October, 2017, after assuming the position of researcher at GCOE (Cybernics), University of Tsukuba, researcher at Mechanical Systems Engineering, Graduate School of Nagoya University and Assistant Professor at College of Science and Engineering, Aoyama Gakuin University. He is engaged in studies on ubiquitous power generating system, autonomous distributed control, robotic sensor network, biosignal process, automatic assembly via robot. He is a member of IEEE, Robotics Society of Japan, Society of Instrument and Control Engineers, Japan Society of Mechanical Engineers, Virtual Reality Society of Japan. He received Advanced Robotics Best Paper Award, FA Foundation Dissertation Award.

AUTHORS (continued) (from left to right)

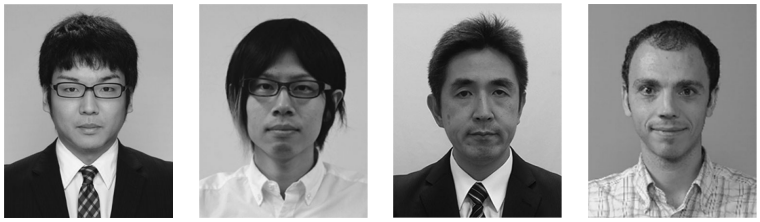

Yusuke Kobana (nonmember) graduated (Department of Integrated Information Technology, College of Science and Engineering, Aoyama Gakuin University) in 2014. He completed Master's program (Graduate School of Science and Engineering of its university) in 2016. He is now working for Canon, Inc. since 2016. He is engaged in studies on mobile sensing, participatory sensing.

Naoya Isoyama (nonmember) graduated (Electrical and Electronics Engineering of Kobe University) in 2010. He completed Master's program of its Graduate School of Engineering in 2012. He completed doctorate program of its Graduate School of Engineering in 2015. He is now Assistant Professor at College of Science and Engineering, Aoyama Gakuin University. He is engaged in studies on wearable computing, entertainment computing.

Yoshito Tobe (member) was a Professor at Integrated Information Technology, College of Science and Engineering, Aoyama Gakuin University in 2012 after pursuing careers at Toshiba, Keio University, Tokyo Denki University. He is exploring studies on sensor network, participatory sensing. He is a member of IEEE, Society of Instrument and Control Engineers, Institute of Electronics, Information and Communication Engineers, Academy of Human Informatics.

Guillaume Lopez (nonmember) completed doctorate program (Department of Human and Engineered Environmental Studies, Graduate School of Frontier Sciences, University of Tokyo) in 2005. He is a Doctor of Environmentology. He is now an Associate Professor at College of Science and Engineering, Aoyama Gakuin University since April 2013 after pursuing careers at Nissan Motors Corporation, as a researcher at Advanced Mobility Research Center, as a Specially Appointed Assistant Professor at Faculty of Engineering, University of Tokyo. He is engaged in studies on the comprehensive technology encompassing wearable sensing, user interface, and information system for improvement of QOL healthcare.